# Supplementary Methods

## Cell Culture

MDA-MB-435-GFP (AntiCancer Inc., San Diego. Cells were maintained in DMEM high glucose supplemented with 10% FBS + 200 μg/ml G418 (Gibco) (1). Cells were sub-cultured for at least three passages before harvesting at their linear growth phase (approximately 70-80% confluent) for mammary fat pad (m.f.p.) injection.

## Drugs and Reagents

For tumor treatment, rapamycin, paclitaxel and anti-VEGF neutralizing antibody were purchased from LC laboratories, Bedford laboratories, or R&D Systems, respectively. Paclitaxel-BODIPY $^{564/570}$ and Angiosense$^{750}$ probes were obtained from Invitrogen and VisEn, respectively. Lectin was obtained from Vector Laboratories. Antibodies used for immunofluorescence and immunohistochemistry were purchased from the following commercial sources: CD31 (BD), α-SMA (ABCAM), NG2 (ABCAM), and Ki-67 (DAKO).

## Treatment of Tumors in Athymic Mice

All animal studies were carried out according to protocols approved by IACUC Committee at the University of Chicago. Female athymic Ncr/nu mice (Frederick), 4-6 weeks old, 18 to 20 g, were used in the study. For tumor transplantation, $5x10^6$ cultured MDA-MB-435-GFP cells, suspended in 0.1 ml of PBS and were injected into the left inguinal mammary fat pad. Tumor growth was measured twice weekly by calipers and tumor volume calculated. Drug treatment was initiated when the tumor volume reached ~200 to 250 $mm^3$. For determining the therapeutic efficacy of rapamycin and anti-human VEGF antibody, tumor-bearing animals were randomly divided into 3 treatment groups of 6-7

animals as indicated. Rapamycin, freshly dissolved in diluents with 5.2% Tween 80 and 5.2% PEG, was administrated daily i.p. at 5 mg/kg /day for 2 weeks. Anti-VEGF neutralizing antibody (5 μg/kg) was given i.p. three times a week for two weeks. Control mice were given equal volumes of PBS. At the end of the treatment on day 14, animals were sacrificed and tumor tissues were weighed. Tumor samples were collected, either frozen and embedded in optimal cutting temperature compound (OCT, Tissue-Tek) for immunofluorescence staining and analysis; or fixed in 10% formalin and paraffin-embedded for immunohistochemistry analysis; or snap frozen in liquid nitrogen for future quantitative PCR and gene array analysis.

For vessel normalization and combination chemotherapy, m.f.p tumor-bearing mice were randomly divided into four treatment groups: 1) Normalization regimen: anti-VEGF antibody (5 μg/kg) was given three times (i.p.) for the first week, followed by treatment with paclitaxel (15 mg/kg) three times a week for two additional weeks; 2) anti-VEGF antibody alone regimen: anti-VEGF antibody (5 μg/kg) was given three times (i.p.) for the first week, followed by treatment with vehicle (PBS) three times a week for two additional weeks; 3) Paclitaxel alone regimen: PBS was given (i.p.) three times for the first week, followed by treatment with paclitaxel (15 mg/kg) three times a week for two additional weeks; 4) Vehicle control: Control tumor-bearing animals were given PBS (i.p.) three times a week for three weeks (Treatment schedule see Figure 4b). The dose of paclitaxel and the treatment schedule were determined as previously described (2, 3).

**Real-time Imaging of Tumor Angiogenesis and Response to Therapy**

The Olympus OV100 Small Animal Imaging System was used for real-time noninvasive imaging of MDA-MD-435 tumors in the mammary fat pad. The optics of the OV100 fluorescence

imaging system have been optimized for high light-gathering capacity providing a 105-fold magnification range for seamless imaging of the entire body down to the subcellular level without disturbing the animal. The OV100 is equipped with GFP, RFP, and near-infrared (NIR) fluorescence filter sets enabling multi-channel co-imaging (4, 5). To prepare the animals for imaging, mice were anesthetized with a mixture of ketamine and xylazine. For conducting dual-channel imaging with BODIPY 564/570-paclitaxel and with the near inferred (NIR) blood pool agent AngioSense$^{750}$, the probes were injected via the tail vein 4h before imaging (20 nmol/mouse and 2 nmol/mouse, respectively). Eight-bit planer images were acquired through the RFP and 750 nm channels of the OV100 [7]. GFP Z-stacks from tumor imaging were obtained between 2-4 mm at 10-μm steps at the 1.6x zoom level. Image analysis was performed by compiling the Z-stack into a 3-dimensional projection image using ImageJ (NIH) (see below for details).

**Image Processing and Analysis**

Stack image series were aligned using Stackreg NIH ImageJ plugin. Background was subtracted (rolling ball or bandpass FFT), and stacks were used to create extended depth of field composites or three-dimensional projections. Red-cyan anaglyphs were created from 3D projections with 5-10 degrees difference of perspective. Some images were filtered with unsharp mask to enhance edges of vessels.

**Quantitative Measurement of Tumor Vessel Density Using FMT Imaging**

The VisEn FMT1 imaging system enables tomographic slicing and quantification of fluorochrome concentration and distribution with sub-millimeter spatial resolution and picomolar sensitivity. The FMT1 system is optimized for probes coupled with either 680 nm or the 750 nm

channels. The FMT1 system was used for quantifying tumor vessel density in live mice by measuring the tumor uptake of the blood pool probe AngioSense$^{750}$ (VisEn) at 4 h post tail-vein injection. 150 µl (2 nmol fluorochrome) of AngioSense$^{750}$ (VisEn) were injected intravenously. Control, rapamycin-treated and anti-VEGF antibody-treated mice were imaged on days 0, 7, and 14 during the course of treatment. Anesthetized mice were positioned in the imaging chamber. Coronal fluorescence-mediated tomography images were acquired using a continuous wave-type scanner capable of acquiring transillumination, reflectance, and absorption data (VisEn) (6). Images were acquired by scanning through the mouse body. Image data sets were reconstructed on a personal computer by using FMT 3.0 software. Images were displayed as raw data sets and as reconstructed three-dimensional data sets in transverse, sagittal, and coronal planes. Fluorochrome concentration in the target was automatically calculated from reconstructed images and expressed as picomols fluorochrome per defined target volume.

**Immunofluorescence and Immunohistochemistry Staining and Characterization**

For immunohistochemistry analysis, 5 micron-cut paraffin-embedded tumor sections were deparafinized, hydrated and H&E stained or immunoassayed using the avidin-biotin immunoperoxidase (Vector Laboratories, Burlingame, CA) method[5]. Images were captured and analyzed using the Zeiss Axioscope microscope.

For immunofluorescence staining, OCT-embedded frozen tumor tissues were cut into 10 µM or 60 µM sections, air dried and stored at -80°C until staining was performed. Cryosections were warmed to room temperature for 30 min, and fixed in ice-cold acetone at -20°C for 10 min. Then slides were incubated in blocking solution (10% goat serum in 0.1% Triton X-100 PBS) for 1h

followed by incubation with the first primary antibody (CD31, BD Pharmingen; α–SMA, ABCAM; and NG2, Millipore) diluted 1:100 in blocking solutions at 4°C overnight. After washing, slides were incubated with the fluorophore-labeled secondary antibody (Molecular Probes), diluted 1:400 in blocking solution, for 30 min at room temperature. For vessel staining, 20 μg/ml of fluorescein-labeled tomato lectin (Vector Laboratories) was applied to frozen-section slides which were incubated at 4°C overnight. The slides were then mounted in Vectashield mounting medium with 4', 6-diamidino-2-phenyl- indole (Vector Laboratories). Images were captured and analyzed using the Zeiss Axiovert 200 and Leica SP-2 confocal microscope.

**Quantification of Mitotic Figures and Karyolitic Cancer Cells.**

Five-micron sections were cut from paraffin embedded MDA-MB-435 tumor tissue, deparafinized, rehydrated and stained with hematoxylin and eosin (H&E).

Mitotic figures in the non-necrotic epithelial component of tumor tissue were counted in 50 random selected fields for each tumor through a 40x objective lens, using a Lietz light microscope. The average mitotic figure count per field was calculated for each tumor and then for 5 tumors from each treatment group (i.e. a total of 250 random fields were scored for each treatment). Similarly, cancer cells that exhibited karyolysis were counted under 1000x magnification. 10 random fields were counted from each tumor. A total of 5 tumors (50 high power field) from each treatment group were used for the quantitative and statistical analysis.

The p-values were determined using a single non-parametric Kruskal-Wallis test for all counts across all groups. A p-value <5% was considered significant. This test was followed by the

non-parametric Dunn's Multiple Comparison Test comparing all pairs of groups conducted with the statistical software Graphpad Prism version 4.03.

**Quantitative RT-PCR Analysis of mRNA Expression.**

Total RNAs from MDA-MB-435 tumors were extracted and purified using TRIzol (Gibco/BRL) according to the manufacturer's instructions.

mRNA expression of genes of interest was measured by real-time quantitative PCR carried out using the Applied Biosystems 7900 Sequence Detector System (Applied Biosystems). Briefly, random primer first-strand cDNA synthesis was carried out with 1.0 μg of total RNA from tumors using the High Capacity cDNA Reverse Transcription Kit (Invitrogen), Cat#4368814). The mix was incubated at 25°C for 10 min, 37°C for 120 min and 85°C for 5 seconds. cDNA corresponding to approximately 5-10 ng of initial RNA was used for each qPCR reaction. Amplification of genes of interest was performed with Sybr Green qPCR assays using custom designed primers. Mouse specific primers for α-SMA were designed using Invitrogen D-LUX™Designer (https://orf.invitrogen.com/lux/). Sequences were as follows: TAATGGTTGGAATGG GCCAAA (forward), and CGCTGCGTGTTCTATCGGATACTTCAGCG (reverse). Cycle parameters for the PCR reaction were 95°C for 10 minutes followed by 40 cycles of a denaturing step at 95°C for 15 seconds and an annealing/extension step at 60°C for 60 seconds. All reactions including no-reverse transcriptase controls were run in triplicate. The mean Ct was calculated from the triplicates and used for the calculation of RQ. The qPCR condition for each gene was optimized so that the standard error among the triplicates was <0.15Ct. Human TATA-binding protein (TBP) was used as the endogenous control for data normalization. The fold changes of target genes were calculated using the ΔΔCt

method of relative comparison. Quantitative mRNA expression data were acquired and analyzed in either 96- or 384-well-plate format using an Applied Biosystems 7900 Sequence Detector System (Applied Biosystems).

## Literature cited


1. Li, X.*, et al.* Optically imageable metastatic model of human breast cancer. *Clin Exp Metastasis* **19**, 347-350 (2002).
2. Cao, Q.*, et al.* Evaluation of biodistribution and anti-tumor effect of a dimeric RGD peptide-paclitaxel conjugate in mice with breast cancer. *Eur J Nucl Med Mol Imaging* **35**, 1489-1498 (2008).
3. Volk, L.D.*, et al.* Nab-paclitaxel efficacy in the orthotopic model of human breast cancer is significantly enhanced by concurrent anti-vascular endothelial growth factor A therapy. *Neoplasia* **10**, 613-623 (2008).
4. Yamauchi, K.*, et al.* Development of real-time subcellular dynamic multicolor imaging of cancer-cell trafficking in live mice with a variable-magnification whole-mouse imaging system. *Cancer Res* **66**, 4208-4214 (2006).
5. Zhang, Q.*, et al.* The role of the intravascular microenvironment in spontaneous metastasis development. *Int J Cancer* **126,** 2534-2541 (2009).
6. Montet, X.*, et al.* Tomographic fluorescence imaging of tumor vascular volume in mice. *Radiology* **242**, 751-758 (2007).

**rapamycin**

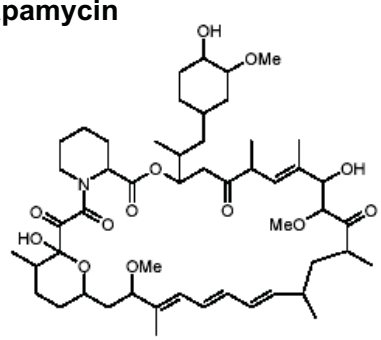

$C_{51}H_{79}NO_{13}$ **MW: 914.2**

http://www.fermentek.co.il/rapamycin.htm

**paclitaxel**

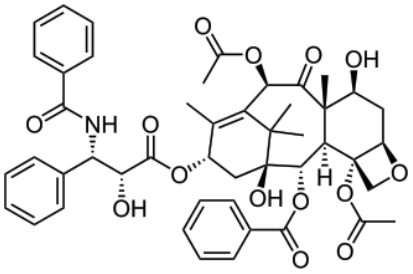

$C_{47}H_{51}NO_{14}$ **MW: 853.9**

http://en.wikipedia.org/wiki/Paclitaxel

**paclitaxel, BODIPY® 564/570 conjugate**

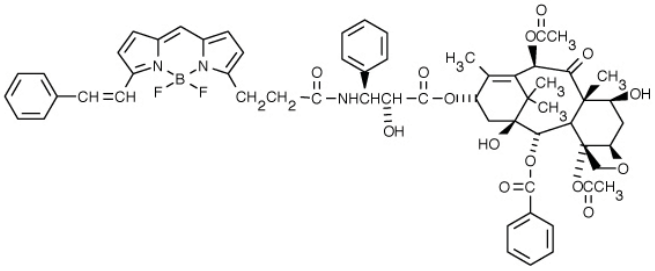

$C_{60}H_{63}BF_2N_3O_{14}$ **MW: 1099.0**

http://products.invitrogen.com/ivgn/product/P7501

**Supplementary Figure 1. Chemical structures of anti-cancer drugs used in the study**

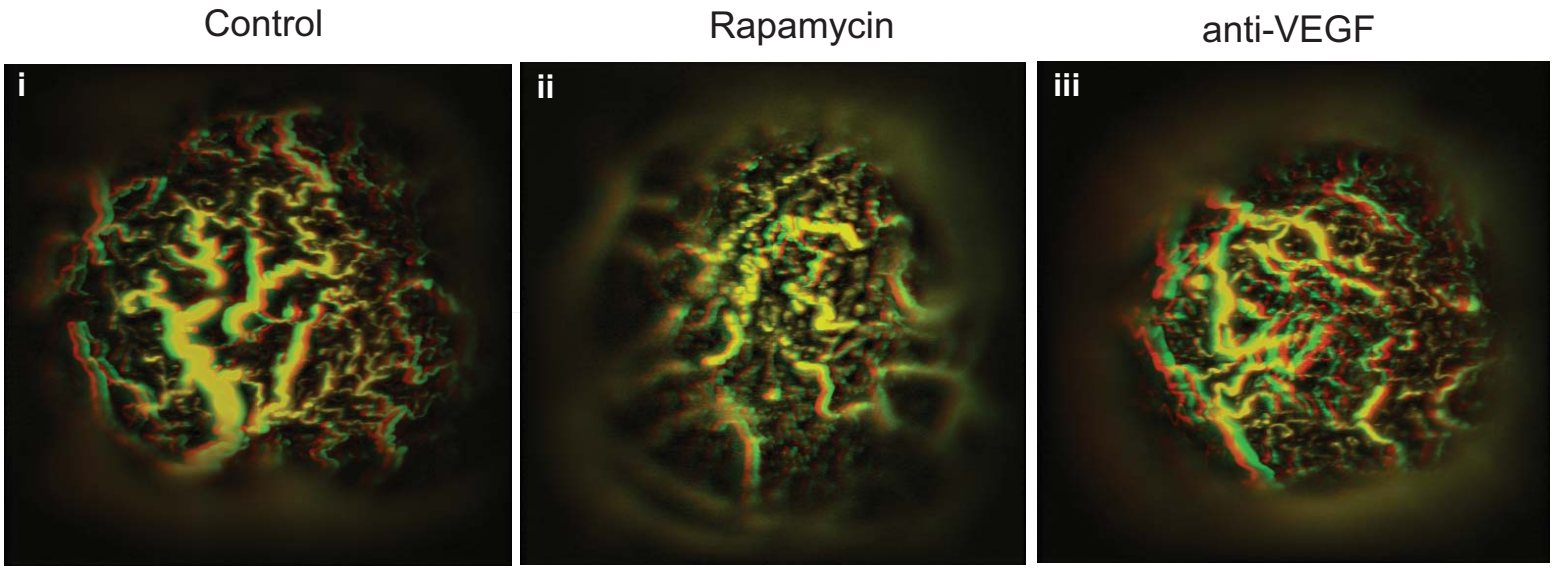


**Supplementary Figure 2. 3D visualization of changes in MDA-MB-435 tumor vascular network upon anti-angiogenic therapies.** In the MDA-MB-435-GFP mammary fat tumors, the non-luminous capillaries were clearly and noninvasively visible as sharply-defined dark networks against the very bright tumor green fluorescence. High-resolution microscopic resolution Z-stack images of tumor micro-vessels were obtained noninvasively through the skin without the requirement of a blood vessel-enhancing contrast agent (Supplementary Methods). Stack image series were aligned using Stackreg NIH ImageJ plugin, background was subtracted (rolling ball or bandpass FFT) and then images were contrast inverted (3D renderings were viewed as bright features of interest against a black background). Stack dimensions were calibrated to correct voxel sizes, and volumes were rendered as standard, varying-angle maximum intensity projections. Red-Green 3D anaglyphs were prepared by 3D rendering two views with 6-10 degree displacement and color-coding these into red and green image channels. The 3D detail is readily appreciated using standard red-blue/cyan stereo glasses. A rapamycin-treated tumor (ii) and a anti-VEGF antibody-treated tumor (iii) showed 3-D morphological evidence of vessel damage (e.g. disjoint vascular network) and of significantly reduced vascular volume compared with the control tumor (i).

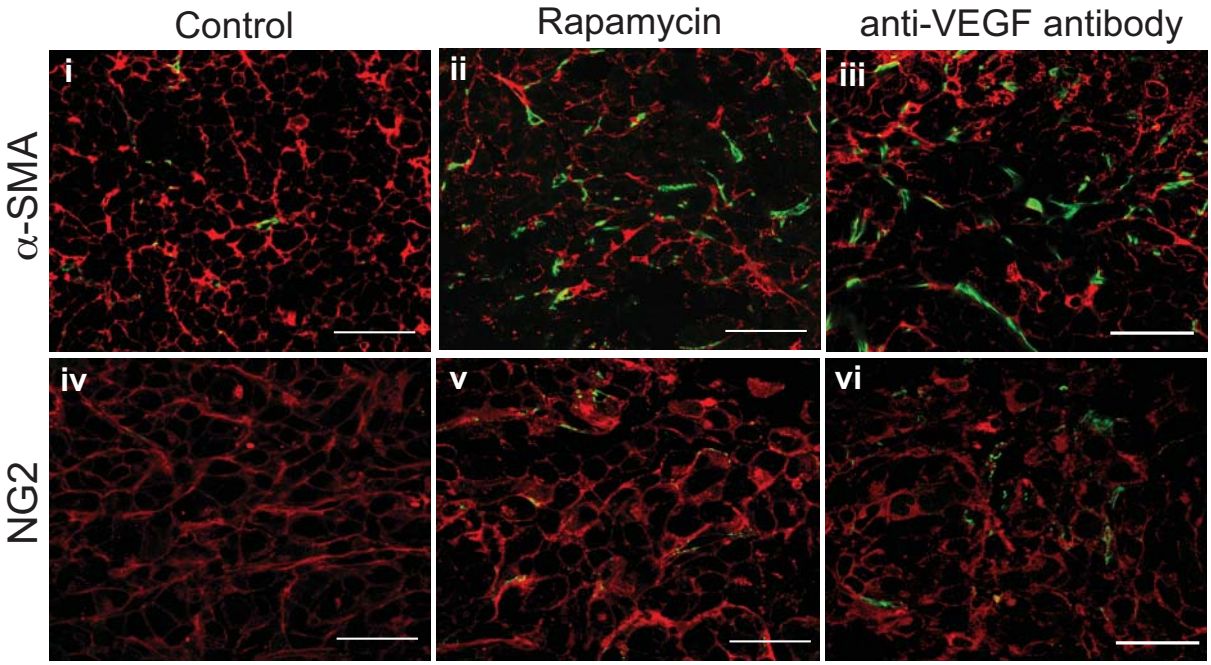


**Supplementary Figure 3. Anti-angiogenic treatment improved tumor vascular hyperpermeability and increased pericyte coverage of tumor vessels.** Lectin angiograms were performed to highlight viable tumor vessels (red). Expression markers for pericytes were determined in control and treated tumors via immuno-fluorescence analysis (green) staining. An increase in α-SMA positive mature pericytes after drug treatments (ii-iii) was confirmed by an increase of NG2 immunofluorescence staining (green), a specific marker for less mature pericytes (iv-vi). Scale bars: 200 μm. Related to Figure 3c.

**Supplementary Movie 1. Visualization of pulsatile blood flow in tumor capillaries via Z-stack images acquired through OV-100 time-course imaging of tumor vasculature in live mice.** In the MDA-MB-435-GFP mammary fat tumors, the non-luminous capillaries were clearly and noninvasively visible as sharply-defined dark networks against the very bright tumor green fluorescence. High-resolution microscopic resolution Z-stack images of tumor microvessels were obtained noninvasively through the skin without the requirement of a blood vessel-enhancing contrast agent (Supplementary Methods). Stack image series were aligned using Stackreg NIH ImageJ plugin and background was subtracted (rolling ball or bandpass FFT). The top-down focal planes were assembled into a movie [20 frames per sec] for a portion of the Z stack where vessel details remained in similar focus. Red arrows indicate regions with pulsatile blood flow in the capillaries.